INTERNATIONAL JOURNAL FOR NUMERICAL METHODS IN FLUIDS
Int. J. Numer. Meth. Fluids 2004; **46**:183–201 (DOI: 10.1002/fld.752)

A stabilized finite element method for the Stokes problem based on polynomial pressure projections

Clark R. Dohrmann[1,*,†] and Pavel B. Bochev[2,‡]

[1]*Structural Dynamics Research Department, Sandia National Laboratories, Mail Stop 0847, Albuquerque, New Mexico, 87185-0847, U.S.A.*
[2]*Computational Mathematics and Algorithms Department, Sandia National Laboratories, Mail Stop 1110, Albuquerque, New Mexico, 87185-1110, U.S.A.*

SUMMARY

A new stabilized finite element method for the Stokes problem is presented. The method is obtained by modification of the mixed variational equation by using local L^2 polynomial pressure projections. Our stabilization approach is motivated by the inherent inconsistency of equal-order approximations for the Stokes equations, which leads to an unstable mixed finite element method. Application of pressure projections in conjunction with minimization of the pressure–velocity mismatch eliminates this inconsistency and leads to a stable variational formulation.

Unlike other stabilization methods, the present approach does not require specification of a stabilization parameter or calculation of higher-order derivatives, and always leads to a symmetric linear system. The new method can be implemented at the element level and for affine families of finite elements on simplicial grids it reduces to a simple modification of the weak continuity equation. Numerical results are presented for a variety of equal-order continuous velocity and pressure elements in two and three dimensions. Copyright © 2004 John Wiley & Sons, Ltd.

KEY WORDS: Stokes equations; stabilized mixed methods; equal-order interpolation; inf–sup condition

1. INTRODUCTION

The focus of this study is a stabilized finite element method for the Stokes problem based on local L^2 polynomial pressure projections. The projections are introduced to address a fundamental inconsistency present for elements employing equal-order approximation of velocity and pressure.

*Correspondence to: C. R. Dohrmann, Sandia National Laboratories, Mail Stop 0847, Albuquerque, New Mexico, 87185-0847, U.S.A.
†E-mail: crdohrm@sandia.gov
‡E-mail: pbboche@sandia.gov

Contract/grant sponsor: United States Department of Energy's National Nuclear Security Administration; contract/grant number: DE-AC-94AL85000

Published online 23 June 2004

Received 18 December 2003
Revised 10 May 2004

The origins of this inconsistency can be explained by inspecting the mixed variational form of the Stokes equations. There, stability of the weak equations results from a special relationship between the velocity and pressure spaces, which ensures that the pressure space coincides with the range of the divergence operator. One can show that (see Reference [1, p. 81]) this special relationship is equivalent to the inf–sup condition [2]. It is well-known that a discrete version of this condition is necessary and sufficient for stable mixed finite element approximations of the Stokes problem; see References [2, 1], or Reference [3]. A discrete inf–sup condition forces pressure and velocity finite element spaces into a relationship that mimics the continuous case. Because for equal-order finite element pairs the range of the divergence is a piecewise polynomial space of one degree less than the pressure space, it is intuitively clear that such pairs will never satisfy the discrete inf–sup condition.

The same inconsistency exists for equal-order approximations of compressible problems, where pressure is proportional to the divergence of the velocity. For example, in a six-node triangular element with quadratic approximation of velocity and pressure, the spatial variation of pressure is linear rather than quadratic as implied by the element formulation.

These observations prompt application of element based pressure projections in the mixed bilinear form as a way to eliminate the approximation inconsistency. This idea can be further justified by noting that there is no such inconsistency for the stable Taylor–Hood (P2-P1) element formulation. However, it is clear that elimination of the pressure–velocity inconsistency alone may not be enough to ensure stable approximation, because a pair such as P1-P0 is formally 'consistent', but unstable. Thus, in our stabilization approach we supplement local pressure projections by an additional term that penalizes pressure deviations from the 'consistent' polynomial order. Our new method combines these two modifications of the mixed bilinear form to provide a finite element formulation of the Stokes problem that remains stable and accurate for all equal-order velocity–pressure pairs.

The new stabilized method for the Stokes problem differs from existing approaches in several important aspects. Unlike *consistently* stabilized methods; see References [4–9], and the *weakly consistent* method of Bochev and Gunzburger [10], stabilization in our method is accomplished without the use of the momentum equation residual. This eliminates the need to calculate higher-order derivatives, to provide for their approximation in the lowest-order case[§] [11], and to specify a mesh-dependent stabilization parameter. Our method also retains the symmetry of the original mixed problem. The only residual based stabilization that has the same property is the Galerkin least-squares method [6]. However, this method is conditionally stable and requires careful selection of the mesh-dependent parameter; see Reference [12].

A non-residual based stabilized method, motivated by fractional step algorithms for time-dependent problems, has been proposed and studied in References [13–15]. This method introduces the projection of the pressure gradient onto the velocity space as a new dependent variable and uses the difference between these two fields to relax the continuity equation. While this approach has some similarity with our method, it still requires a choice of mesh-dependent parameters, and leads to larger algebraic problems. Another important difference is that pressure gradient projections into the velocity space are not local because this space is

[§]The problems with approximation of the second order terms in the momentum equation residual can be avoided by reformulation of the problem as a first-order system. An example is the velocity–pressure–stress method of Behr *et al*. [8]. However, this approach increases the number of the dependent variables by 3 and 6 in 2 and 3 dimensions, respectively.

continuous, while our method employs projections into a discontinuous space and thus, can be implemented at the element level.

Another example of non-residual based stabilization is the local and global pressure jump formulation for Q1-P0 quadrilateral elements [16]. It is based on the idea of *filtering* the spurious modes that pollute this particular finite element pair. Use of projections onto macroelement spaces has been proposed for stabilization of Q1-P0 and P1-P1 elements [17]. The present method of stabilization involves polynomial projections over individual elements rather than macroelements. As a result, the need for mesh decompositions into macroelements is avoided.

Penalty methods are another category of non-residual based regularizations; see [18–21]. They, however, differ from stabilized methods in the sense that application of a penalty does not circumvent the inf–sup condition and only serves to uncouple pressure from velocity. In this sense, penalty methods should be viewed as solution, rather then stabilization procedures for the mixed equations.

The formulation of the stabilized method is presented in Section 2 following an introduction to the nomenclature. Implementation details are presented in Section 3 and numerical results are given in Section 4. Although numerical results are presented only for equal-order continuous velocity and pressure elements, polynomial projections can also be used to stabilize discontinuous pressure elements such as Q1-P0 and P1-P0. The stabilization, however, is node-based rather than element-based. Formal error and stability analysis of the method will be the subject of the forthcoming paper [22].

1.1. Nomenclature

In what follows, Ω denotes a simply connected bounded region in $\mathbb{R}^d$, $d=2,3$, with a Lipschitz continuous boundary Γ. Throughout the paper, we employ the usual notation $H^l(\Omega)$, $\|\cdot\|_l$, $(\cdot,\cdot)_l$, $l\geqslant 0$, for the Sobolev spaces of all functions having square integrable derivatives up to order l on Ω, and the standard Sobolev norm and inner product, respectively. When $l=0$ we will write $L^2(\Omega)$ instead of $H^0(\Omega)$ and drop the index from the inner product designation. As usual, $H_0^l(\Omega)$ will denote the closure of $C_0^\infty(\Omega)$ with respect to the norm $\|\cdot\|_l$ and $L_0^2(\Omega)$ will denote the space of all square integrable functions with vanishing mean. Spaces consisting of vector-valued functions will be denoted in bold face.

In this paper, we consider methods for the Stokes equations that use pressure and velocity finite element spaces of the same polynomial order and defined with respect to the same partition $\mathscr{T}_h$ of Ω into finite elements Ω_e. For instance, Ω_e can be a hexahedron or a tetrahedron in three dimensions, or a triangle or a quadrilateral in two dimensions. Let k be a non-negative integer number. For simplicial elements we consider affine families of Lagrange finite element spaces

$$P_k=\{u^h\in C^0(\Omega)\,|\,u^h_{|_{\Omega_e}}\in\mathscr{P}_k(\Omega_e);\ \forall\Omega_e\in\mathscr{T}_h\} \tag{1}$$

where $\mathscr{P}_k(\Omega_e)$ is the space of complete polynomials of degree k defined on the element Ω_e.

For quadrilateral and hexahedral elements we consider the Lagrange spaces

$$Q_k=\{u^h\in C^0(\Omega)\,|\,u^h_{|_{\Omega_e}}=\hat{u}^h\circ F^{-1};\ \hat{u}^h\in\mathscr{Q}_k(\hat{\Omega}_e)\} \tag{2}$$

where $\hat{\Omega}_e$ is a reference element, $F:\hat{\Omega}_e\mapsto\Omega_e$ is a bilinear or trilinear mapping, and $\mathscr{Q}_k$ is the space of all polynomials on $\hat{\Omega}_e$ whose degree does not exceed k in each co-ordinate direction.

Note that unless Ω_e is a parallelogram or a parallelepiped, u^h is not a piecewise polynomial function. For simplicity, unless there is a need to distinguish between simplicial and non-simplicial elements, we will use the symbol R_k to denote both kinds of finite element spaces. In keeping with our earlier convention, vector valued finite element spaces will be denoted in bold face, e.g. $\mathbf{R}_k$.

To define the stabilized method we will need an L^2 projection operator onto the discontinuous polynomial space

$$[P_m] = \{q^h \in L^2(\Omega) \,|\, q^h_{|\Omega_e} \in \mathscr{P}_m(\Omega_e); \quad \forall \Omega_e \in \mathscr{T}_h\} \tag{3}$$

where m is a non-negative integer number. In (3) $\mathscr{T}_h$ can be a simplicial or a non-simplicial partition of Ω into finite elements. Given a function $q \in L^2(\Omega)$ the projection operator ρ_m: $L^2(\Omega) \mapsto [P_m]$ is defined by

$$\rho_m q = q^h \in [P_m]$$

if and only if

$$\int_\Omega r^h(\rho_m q - q)\,\mathrm{d}\Omega = 0 \quad \forall r^h \in [P_m] \tag{4}$$

We recall that for a $p \in L^2(\Omega)$,

$$\rho_m p = \operatorname{argmin} \frac{1}{2} \int_\Omega (\rho_m q - p)^2\,\mathrm{d}\Omega$$

Equation (4) is a necessary condition for the minimizer of this functional. Because $[P_m]$ is discontinuous, (4) uncouples into local element problems

$$\int_{\Omega_e} r^h(\rho_m q - q)\,\mathrm{d}\Omega_e = 0 \quad \forall r^h \in \mathscr{P}_m(\Omega_e); \;\; \forall \Omega_e \in \mathscr{T}_h \tag{5}$$

which can be solved independently of each other at the element level.

2. FORMULATION OF THE STABILIZED METHOD

We consider the incompressible Stokes problem

$$-\nu \Delta \mathbf{u} + \nabla p = \mathbf{f} \quad \text{in } \Omega \tag{6}$$

$$\nabla \cdot \mathbf{u} = 0 \quad \text{in } \Omega \tag{7}$$

augmented with the homogeneous velocity boundary condition

$$\mathbf{u} = 0 \quad \text{on } \Gamma \tag{8}$$

We assume ν is a positive constant.

The mixed variational form of (6)–(8) is to seek $(\mathbf{u}, p) \in \mathbf{H}_0^1(\Omega) \times L_0^2(\Omega)$ such that

$$Q(\mathbf{u}, p; \mathbf{v}, q) = F(\mathbf{v}, q) \quad \forall (\mathbf{v}, q) \in \mathbf{H}_0^1(\Omega) \times L_0^2(\Omega) \tag{9}$$

where

$$\begin{aligned} F(\mathbf{v}) &= \int_\Omega \mathbf{f} \cdot \mathbf{v} \, \mathrm{d}x \\ Q(\mathbf{u}, p; \mathbf{v}, q) &= A(\mathbf{u}, \mathbf{v}) + B(\mathbf{v}, p) + B(\mathbf{u}, q) \end{aligned} \tag{10}$$

and

$$A(\mathbf{u}, \mathbf{v}) = \int_\Omega \nu \nabla \mathbf{u} : \nabla \mathbf{v} \, \mathrm{d}\Omega, \quad B(\mathbf{v}, p) = -\int_\Omega p \nabla \cdot \mathbf{v} \, \mathrm{d}\Omega \tag{11}$$

To approximate (6)–(8) we consider the equal-order pair (V^h, S^h) where

$$V^h = \mathbf{R}_k \cap \mathbf{H}_0^1(\Omega) \quad \text{and} \quad S^h = R_k \cap L_0^2(\Omega) \tag{12}$$

Such a pair does not satisfy the inf–sup condition and restriction of (9) to (V^h, S^h) will result in an unstable method. To stabilize the mixed form (10) we consider the projection operator ρ_{k-1}, the bilinear form

$$C(p^h, q^h) = \int_\Omega \frac{1}{\nu} (p^h - \rho_{k-1} p^h)(q^h - \rho_{k-1} q^h) \, \mathrm{d}\Omega \tag{13}$$

and modify (10) to

$$\tilde{Q}(\mathbf{u}^h, p^h; \mathbf{v}^h, q^h) = A(\mathbf{u}^h, \mathbf{v}^h) + B(\mathbf{v}^h, \rho_{k-1} p^h) + B(\mathbf{u}^h, \rho_{k-1} q^h) - C(p^h, q^h) \tag{14}$$

The stabilized method is to seek $(\mathbf{u}^h, p^h)$ in $V^h \times S^h$, such that

$$\tilde{Q}(\mathbf{u}^h, p^h; \mathbf{v}^h, q^h) = F(\mathbf{v}^h, q^h) \quad \forall (\mathbf{v}^h, q^h) \in V^h \times S^h \tag{15}$$

Application of the projection operator to the pressure test and trial functions serves to remove the approximation inconsistency present for equal-order velocity and pressure spaces. The role of the form $C(\cdot, \cdot)$ is to further penalize pressure variation away from the range of the divergence operator. This last term is crucial for the stability of the new method.

2.1. The method for affine finite element spaces

Let us consider a simplicial partition $\mathscr{T}_h$ and an affine family of finite element spaces R_k. We recall that such elements are affine equivalent to a single reference element [23, p. 87] and so their nodes must be affine images of the reference element nodes. For example, if six-node quadratic elements are used, the mid-edge nodes of each triangle must be centred. The same applies to higher order Lagrange elements.

On each element V^h consists of functions that are complete polynomials of degree k. In this case the divergence of a field $\mathbf{v}^h \in V^h$ is a discontinuous piecewise polynomial function whose degree on each element does not exceed $k-1$, that is,

$$\nabla \cdot \mathbf{v}^h \in [P_{k-1}], \quad \forall \mathbf{v}^h \in V^h$$

Using definition (4) of the projection operator, it is not hard to see that

$$\int_\Omega (q^h - \rho_{k-1} q^h) \nabla \cdot \mathbf{v}^h \, \mathrm{d}\Omega = 0$$

for any $\mathbf{v}^h$ in V^h. As a result, for simplicial triangulations

$$B(\mathbf{v}^h, \rho_{k-1} q^h) = B(\mathbf{v}^h, q^h) \tag{16}$$

and the modified bilinear form (14) simplifies to

$$\tilde{Q}(\mathbf{u}^h, p^h; \mathbf{v}^h, q^h) = A(\mathbf{u}^h, \mathbf{v}^h) + B(\mathbf{v}^h, p^h) + B(\mathbf{u}^h, q^h) - C(p^h, q^h) \tag{17}$$

Therefore, for simplicial elements our method requires only the addition of the penalty form $C(\cdot, \cdot)$ to the mixed variational equation. The fact that for such elements the method reduces to (17) further highlights the importance of this term in the formulation.

Consider now a case where $\mathscr{T}_h$ is not simplicial. There are two possibilities. If $\mathscr{T}_h$ contains only parallelepipeds or parallelograms the finite element space R_k is again an affine family (assuming that all physical nodes, e.g. mid-edge nodes, are affine images of their reference counterparts). The space V^h will consist of polynomial functions whose degree in each co-ordinate direction does not exceed k. However, in this case the divergence of a field $\mathbf{v}^h \in V^h$ is not a function in $[P_{k-1}]$ and (16) does not hold. To obtain a similar simplification for non-simplicial partitions it is necessary to redefine the range of the projection operator to be the discontinuous piecewise polynomial space $[\nabla \cdot V^h]$. With this modification the stabilized form again reduces to (17).

The second possibility is for $\mathscr{T}_h$ to contain general hexahedral or quadrilateral elements. Then, R_k is not an affine image of a polynomial space and V^h does not contain polynomials. As a result, $\nabla \cdot \mathbf{v}^h$ is not a polynomial function and validity of (16) would require a projection operator whose range is not a polynomial space.

We see that in both cases, that is, affine finite elements on non-simplicial partitions and non-affine elements, it is necessary to redefine the range of the projection operator if a relationship like (16) is desired. This strategy, however, would unduly complicate the method and for this reason it is not pursued here. Instead, we explore another possibility which is to apply projections only in the penalty term. This variant of our method corresponds to using the simplified bilinear form (17) in *all occasions*, including non-affine elements and non-simplicial grids.

2.2. *Connection with optimization problems*

The mixed variational equation (9) is the first-order optimality condition for the saddle-point $(\mathbf{u}, p)$ of the Lagrangian functional

$$L(\mathbf{v}, q) = \frac{1}{2} \int_\Omega \nu |\nabla \mathbf{v}|^2 \, \mathrm{d}x - \int_\Omega q \nabla \cdot \mathbf{v} \, \mathrm{d}x - \int_\Omega \mathbf{f} \cdot \mathbf{v} \, \mathrm{d}x \tag{18}$$

The stabilized problem (15) is also related to an optimization problem. Consider the modified Lagrangian functional

$$\tilde{L}(\mathbf{v}, q) = \frac{1}{2} \int_\Omega \nu |\nabla \mathbf{v}|^2 \, \mathrm{d}\Omega - \int_\Omega \rho_m q \nabla \cdot \mathbf{v} \, \mathrm{d}\Omega - \int_\Omega \mathbf{f} \cdot \mathbf{v} \, \mathrm{d}\Omega - \frac{1}{2} \| \nu^{-1/2} (q - \rho_m q) \|_0^2 \tag{19}$$

Using standard tools from the calculus of variations one can show that the variational equation (15) is the first-order optimality system for this Lagrangian restricted to the finite element pair $V^h \times S^h$.

Not all stabilized methods can be related to an optimization problem. The conditionally stable Galerkin least-squares method [6] is one of the few stabilized methods that correspond to an optimality system for some modification of (18). The pressure-Poisson [10, 5], the Douglas–Wang [7], and the pressure gradient projection method [13] are all examples of stabilized methods that are not associated with an optimization setting. Consequently, these methods cannot be derived starting from a modified Lagrangian functional.

Because the last term in (19) resembles the term that appears in the *penalized* Lagrangian

$$L_\varepsilon(\mathbf{v}, q) = \frac{1}{2}\int_\Omega \nu|\nabla \mathbf{v}|^2 \,\mathrm{d}\Omega - \int_\Omega q\nabla\cdot\mathbf{v}\,\mathrm{d}\Omega - \int_\Omega \mathbf{f}\cdot\mathbf{v}\,\mathrm{d}\Omega - \frac{\varepsilon}{2}\|q\|_0^2 \tag{20}$$

it is of interest to compare the two methods that result from these functionals. Taking first variations of (20) with respect to $\mathbf{v}$ and q gives the weak equation: seek $(\mathbf{u}_\varepsilon, p_\varepsilon)$ in $\mathbf{H}_0^1(\Omega)\times L_0^2(\Omega)$ such that

$$A(\mathbf{u}_\varepsilon, \mathbf{v}) + B(p_\varepsilon, \mathbf{v}) = F(\mathbf{v}) \quad \forall \mathbf{v}\in \mathbf{H}_0^1(\Omega) \tag{21}$$

$$B(q, \mathbf{u}_\varepsilon) = \varepsilon D(p_\varepsilon, q) \quad \forall q \in L_0^2(\Omega) \tag{22}$$

The second equation can be used to eliminate the pressure and to obtain an equation in terms of $\mathbf{u}_\varepsilon$ only

$$A(\mathbf{u}_\varepsilon, \mathbf{v}) + \frac{1}{\varepsilon}\int_\Omega (\nabla\cdot\mathbf{u}_\varepsilon)(\nabla\cdot\mathbf{v})\,\mathrm{d}\Omega = F(\mathbf{v}) \quad \forall \mathbf{v}\in\mathbf{H}_0^1(\Omega) \tag{23}$$

Discretization of (23) gives the classical penalty method for the Stokes equations. Even though the pressure does not enter explicitly in (23), the well-posedness of the penalty problem is still subject to an inf–sup condition between the velocity space V^h and an implicit pressure space induced by the equation $\varepsilon p_\varepsilon = -\nabla\cdot\mathbf{u}_\varepsilon$; see Reference [20] or [21]. If the pair consisting of the velocity space and the induced pressure space is unstable, then the penalty method may fail as $\varepsilon \to 0$. A classical example of such failure is the locking phenomena for linear velocities, where the solution of (23) converges to the trivial solution when $\varepsilon \to 0$.

Instead of first eliminating the pressure and then discretizing (23) we could have started by discretizing the mixed problem (21)–(22) and then eliminate the pressure from the discrete equations. The resulting system would differ from the one obtained by the *eliminate* and *discretize* approach. In either case, however, the penalty approximation will be unstable if the associated mixed equation is not stable. Consequently, the penalty approach cannot be used to stabilize an unstable mixed method and in that sense it cannot be deemed a stabilization procedure. The proper interpretation of the penalty method is that of a solution procedure for the mixed method.

Consider now the stabilized Lagrangian (19). Taking the first variation of (19) with respect to $\mathbf{v}$ and q gives the weak equation: seek $(\mathbf{u}, p)$ in $\mathbf{H}_0^1(\Omega)\times L_0^2(\Omega)$ such that

$$A(\mathbf{u}, \mathbf{v}) + B(\rho_m p, \mathbf{v}) = F(\mathbf{v}) \quad \forall \mathbf{v}\in \mathbf{H}_0^1(\Omega) \tag{24}$$

$$B(\rho_m q, \mathbf{u}) = C(p, q) \quad \forall q \in L_0^2(\Omega) \tag{25}$$

The stabilized method (15) is obtained by restriction of this variational problem to an arbitrary pair $V^h \times S^h$ of finite element spaces for the velocity and the pressure. Besides the absence of a penalty parameter, the principal difference between the penalty formulation (21)–(22) and the stabilized problem (24)–(25) is that the pressure cannot be eliminated from the second equation in (25). The reason is that $C(\cdot,\cdot)$ vanishes for all pressures that are in the range of the projection operator employed in the definition of this form.

3. IMPLEMENTATION

One of the principal strengths of the new stabilized method is that computation of the pressure projections and the penalty form $C(\cdot,\cdot)$ is completely local. As a result, the overhead associated with the stabilization process is small.

To describe implementation details we consider an arbitrary element Ω_e. The element matrix generated by the unstabilized mixed form (9) can be expressed in the block form

$$K_e = \begin{bmatrix} A_e & B_e^{\mathrm{T}} \\ B_e & 0 \end{bmatrix} \tag{26}$$

where the blocks A_e and B_e are obtained from the bilinear forms $A(\cdot,\cdot)$ and $B(\cdot,\cdot)$, respectively. The stabilized version of K_e can be expressed as

$$K_{es} = \begin{bmatrix} A_e & \tilde{B}_e^{\mathrm{T}} \\ \tilde{B}_e & -C_e \end{bmatrix} \tag{27}$$

where $\tilde{B}_e$ is a modified version of B_e obtained from $B(\rho_{k-1}q^h, \mathbf{v}^h)$ and C_e is a symmetric positive semidefinite matrix generated by the bilinear form $C(\cdot,\cdot)$. A varying v can be approximated by a constant value in each element denoted by v_e.

Let us first consider computation of C_e. The pressure in Ω_e is approximated according to

$$p^h(\mathbf{x}) = p_e^{\mathrm{T}}\psi(\mathbf{x}) \tag{28}$$

where p_e is a vector of nodal pressures for the element, $\psi(\mathbf{x})$ is a vector of shape functions from R_k, and $\mathbf{x}$ is the position vector. To compute the L^2 projection of p^h we use the local formula (5). Let the rows of the vector $a(\mathbf{x})$ form a basis for $[P_{k-1}]$ on Ω_e so that on this element

$$\rho_{k-1}\, p^h(\mathbf{x}) = c^{\mathrm{T}} a(\mathbf{x}) \tag{29}$$

A direct calculation shows that

$$\rho_{k-1}\, p^h(\mathbf{x}) = p_e^{\mathrm{T}} E_e^{\mathrm{T}} D_e^{-1} a(\mathbf{x}) \tag{30}$$

where

$$D_e = \int_{\Omega_e} a(\mathbf{x}) a^{\mathrm{T}}(\mathbf{x})\, \mathrm{d}\Omega_e, \quad E_e = \int_{\Omega_e} a(\mathbf{x})\psi^{\mathrm{T}}(\mathbf{x})\, \mathrm{d}\Omega_e \tag{31}$$

To find C_e we substitute (30) and (28) into

$$\frac{1}{v_e}\int_{\Omega_e}(p^h-\rho_{k-1}p^h)(p^h-\rho_{k-1}p^h)\,\mathrm{d}x$$

which is the restriction of $C(p^h,p^h)$ onto Ω_e. A simple but tedious calculation leads to

$$C_e=\frac{1}{v_e}(M_e-E_e^{\mathrm{T}}D_e^{-1}E_e) \tag{32}$$

where

$$M_e=\int_{\Omega_e}\psi(\mathbf{x})\psi^{\mathrm{T}}(\mathbf{x})\,\mathrm{d}\Omega_e \tag{33}$$

A dimensionless stabilization parameter α could be introduced in (32) by replacing $1/v_e$ with α/v_e. This modification is not essential to our method and is not considered here.

Consider next computation of $\tilde{B}_e$. The divergence of $\mathbf{v}^h$ in the element is approximated according to

$$\nabla\cdot\mathbf{v}^h=d^{\mathrm{T}}(\mathbf{x})v_e \tag{34}$$

where v_e is a vector of nodal velocities for the element. To find $\tilde{B}_e$ we substitute this expression and (30) into the restriction

$$-\int_{\Omega_e}\rho_{k-1}p^h\nabla\cdot\mathbf{v}^h\,\mathrm{d}x$$

of $B(\rho_{k-1}p^h,\mathbf{v}^h)$ to Ω_e. This leads to

$$\tilde{B}_e=-E_e^{\mathrm{T}}D_e^{-1}F_e \tag{35}$$

where

$$F_e=\int_{\Omega_e}a(\mathbf{x})d^{\mathrm{T}}(\mathbf{x})\,\mathrm{d}\Omega_e \tag{36}$$

The matrices $\tilde{B}_e$ and C_e can be calculated together with A_e using standard numerical integration procedures for finite elements.

Recall that the unmodified matrix B_e is given by

$$B_e=-\int_{\Omega_e}\psi(\mathbf{x})d^{\mathrm{T}}(\mathbf{x})\,\mathrm{d}\Omega_e \tag{37}$$

From (16) it follows that for simplicial partitions $\mathscr{T}_h$

$$\tilde{B}_e=B_e$$

that is,

$$-\int_{\Omega_e}\psi(\mathbf{x})d^{\mathrm{T}}(\mathbf{x})\,\mathrm{d}\Omega_e=-E_e^{\mathrm{T}}D_e^{-1}\int_{\Omega_e}a(\mathbf{x})d^{\mathrm{T}}(\mathbf{x})\,\mathrm{d}\Omega_e$$

In this case, the element matrix of the stabilized method simplifies to

$$K_{es} = \begin{bmatrix} A_e & B_e^{\mathrm{T}} \\ B_e & -C_e \end{bmatrix} \tag{38}$$

Recall that to obtain the same form of the stabilized element matrix for non-affine and non-simplicial elements would have required a projection operator whose range is the space $[\nabla \cdot V^h]$. Even for a partition consisting of parallelograms or parallelepipeds this entails an expansion of $a(\mathbf{x})$ that is not necessarily beneficial to the method. Consider, for example, rectangular elements in two space dimensions. If $k=2$, then on each element V^h contains functions that are linear combinations of the monomials

$$1, x, y, x^2, xy, y^2, x^2y, xy^2, x^2y^2$$

and we must choose

$$a(\mathbf{x}) = (1, x, y, x^2, xy, y^2, xy^2, x^2y)$$

Note that $a(\mathbf{x})$ and the original biquadratic basis differ only by the higher-order term x^2y^2 and so the polynomial pressure projection will be almost identical to the pressure itself. As a result, a method implemented with this choice of $a(\mathbf{x})$ will most likely be unstable.

In contrast, the definition of ρ_m employed in our method requires the linear basis vector

$$a(\mathbf{x}) = (1, x, y)$$

Besides leading to a simpler and more efficient implementation, this choice also provides for better stabilization because pressure projection eliminates all higher order terms from the pressure field. Thus, instead of changing $a(\mathbf{x})$ we will also consider a variant of our method where B_e is used in place of $\tilde{B}_e$ regardless of the partition type.

4. NUMERICAL RESULTS

The results in this section are for elements based on equal-order interpolation of velocity and pressure. Element types considered for 2D problems include the three node triangle (TRIA3), six node triangle (TRIA6), four node quadrilateral (QUAD4), and nine node quadrilateral (QUAD9). Element types for 3D problems include the four node tetrahedron (TET4), ten node tetrahedron (TET10), eight node hexahedron (HEX8), and 27 node hexahedron (HEX27). The modified bilinear form in (14) was used for all the results shown. Although numerical results for the bilinear form in (17) are different for non-simplicial elements, we observed no difference in convergence rates or qualitative behaviour by replacing $\tilde{B}_e$ with B_e.

The following error norms are used for the investigation of convergence rates

$$e^h_{uL_2} = \|\mathbf{u}^h - \mathbf{u}\|_0 = \sqrt{\sum_{i=1}^{d} \int_\Omega (u_i^h - u_i)^2 \, \mathrm{d}\Omega} \tag{39}$$

$$e^h_{uH_1} = \|\mathbf{u}^h - \mathbf{u}\|_1 = \sqrt{\sum_{i=1}^{d} \int_\Omega \nabla(u_i^h - u_i) \cdot \nabla(u_i^h - u_i)\, \mathrm{d}\Omega} \tag{40}$$

$$e^h_{pL_2} = \|p^h - p\|_0 = \sqrt{\int_\Omega (p^h - p)^2\, \mathrm{d}\Omega} \tag{41}$$

where d is the spatial dimension and (u_i^h, p_i^h) is the finite element approximation of the exact solution (u_i, p).

We recall that; see [1], for all sufficiently smooth $\mathbf{u}$ and p there exist functions $\mathbf{u}_I^h \in V^h$ and $p_I^h \in S^h$, such that

$$\|\mathbf{u}_I^h - \mathbf{u}\|_0 \leqslant Ch^{k+1}\|\mathbf{u}\|_{k+1} \tag{42}$$

$$\|\mathbf{u}_I^h - \mathbf{u}\|_1 \leqslant Ch^{k}\|\mathbf{u}\|_{k} \tag{43}$$

and

$$\|p_I^h - p\|_0 \leqslant Ch^{k+1}\|p\|_{k+1} \tag{44}$$

respectively. If finite element solutions converge at the same rates as the interpolants, we say that the method is optimal. However, our method uses pressure projection into a polynomial space of one degree less than the space used to define S^h, and so, instead of (44), optimal rates for the pressure should be of one degree less than indicated by this bound. In the numerical studies we use spaces R_k with $k=1$ and $k=2$. Therefore, our method will be optimally accurate if

$$e^h_{uL_2} = O(h^2), \quad e^h_{uH_1} = O(h) \text{ and } e^h_{pL2} = O(h) \tag{45}$$

for $k=1$, i.e. for TRIA4, QUAD4, TET4 and HEX8 elements, and

$$e^h_{uL_2} = O(h^3), \quad e^h_{uH_1} = O(h^2) \text{ and } e^h_{pL2} = O(h^2) \tag{46}$$

for $k=2$, i.e. for TRIA6, QUAD9, TET10 and HEX27 elements.

The first example is for a unit square with $v=1$ and the smooth exact solution

$$u_1 = x + x^2 - 2xy + x^3 - 3xy^2 + x^2 y \tag{47}$$

$$u_2 = -y - 2xy + y^2 - 3x^2 y + y^3 - xy^2 \tag{48}$$

$$p = xy + x + y + x^3 y^2 - 4/3 \tag{49}$$

where

$$\mathbf{u} = (u_1, u_2) \tag{50}$$

The values of $\mathbf{u}$ on the boundary of the square are constrained to those given by (47) and (48). To remove the constant pressure mode from the numerical solution,

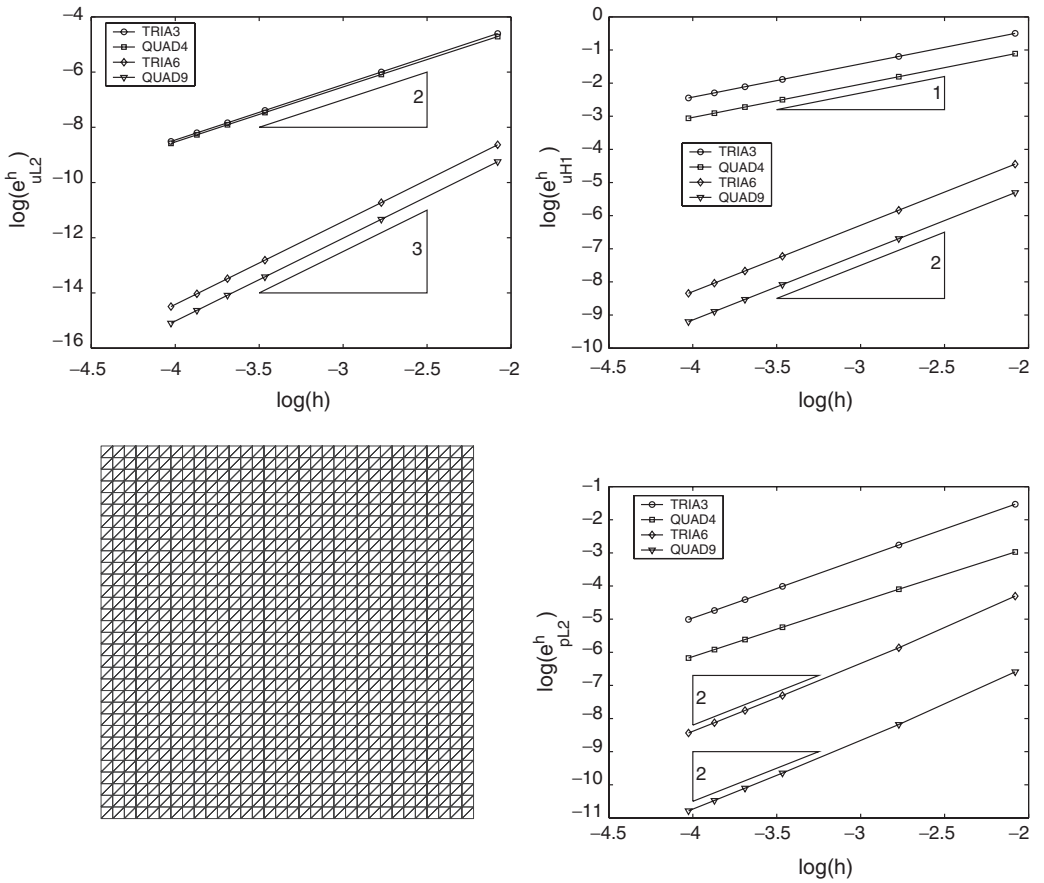

Figure 1. Example triangular mesh and error norms for first example.

the constraint

$$\int_{\Omega} p(\mathbf{x})\,\mathrm{d}\Omega = 0 \tag{51}$$

is also imposed. The term $\mathbf{f}$ is obtained by substituting the exact solution into (6).

Plots of the error norms versus element length h are shown in Figure 1. An example triangular mesh is also shown in the figure. The observed convergence rates for the velocity field are identical with the optimal rates in (45)–(46). For $k=1$ convergence of the pressure error $e^h_{pL_2}$ is better than the expected optimal rate indicated in (45). Instead of line segment slopes near 1, they are between 1.5 and 2. This behaviour was observed for a variety of other exact solutions. Nevertheless, for $k=2$ we see that pressure error does converge according to (46) and so, it seems safe to conclude that the better convergence rate will likely be confined to the lowest order case only.

Table I. Solution errors for different stabilized elements normalized with respect to results for their stable Taylor–Hood counterparts.

$1/h$	etype	$e^h_{uL_2}$	$e^h_{uH_1}$	$e^h_{pL_2}$	e_{div}	etype	$e^h_{uL_2}$	$e^h_{uH_1}$	$e^h_{pL_2}$	e_{div}	$\bar{e}_{\text{div}}$
8	TRIA6	0.999	1.001	3.02	1.000	QUAD9	1.012	1.004	1.36	6.9	0.15
16	TRIA6	1.000	1.000	3.24	1.000	QUAD9	1.004	1.001	1.12	13	0.18
32	TRIA6	1.000	1.000	3.34	1.000	QUAD9	1.001	1.000	1.03	26	0.19
40	TRIA6	1.000	1.000	3.36	1.000	QUAD9	1.001	1.000	1.02	32	0.19
48	TRIA6	1.000	1.000	3.37	1.000	QUAD9	1.001	1.000	1.01	38	0.20
56	TRIA6	1.000	1.000	3.37	1.000	QUAD9	1.000	1.000	1.01	45	0.20

For purposes of comparison, Table I presents the results of Figure 1 for TRIA6 and QUAD9 elements normalized with respect to those of their stable Taylor–Hood counterparts P2-P1 and Q2-Q1, respectively. Also shown in the table are normalized values of the maximum divergence error in an element defined as

$$e_{\text{div}} = \max_e \left| \int_{\Gamma_e} \mathbf{u} \cdot \mathbf{n} \, \mathrm{d}\Gamma_e \right| \tag{52}$$

where Γ_e is the boundary of element e and $\mathbf{n}$ is the unit outward normal of Γ_e. The normalized velocity error norms are very close to unity for both the TRIA6 and QUAD9 stabilized elements. Compared with their stable counterparts, the pressure errors are about three times greater for the TRIA6 element and about the same for the QUAD9 element. The normalized maximum divergence errors are about the same for the TRIA6 and P2-P1 elements. Somewhat unexpected are the significant differences in maximum divergence errors between the QUAD9 stabilized and Q2-Q1 stable elements. On closer examination, it was found that the maximum divergence errors for meshes of Q2-Q1 elements are much lower than those for P2-P1 meshes. The final column in Table I, designated as $\bar{e}_{\text{div}}$, shows QUAD9 results normalized with respect to P2-P1 rather than Q2-Q1. The final two columns in Table I show that the maximum divergence errors for QUAD9 are greater than those for Q2-Q1 but smaller than those for P2-P1. Considering the results in Table I, there is no clear advantage of the stabilized quadratic elements over their stable counterparts in terms of accuracy for this example. The stabilized elements do have the advantage of simpler computer implementation since all nodes have the same degrees of freedom. In addition, some researchers have found that stabilized element formulations can lead to improved performance of iterative solvers, see e.g. Reference [24].

We note that better pressure accuracy for TRIA6 elements and lower maximum divergence errors for QUAD9 elements can be achieved by replacing the constant $1/\nu_e$ in (32) by α/ν_e where α is a positive dimensionless parameter greater than 1 for TRIA6 elements and less than 1 for QUAD9 elements. Although such 'tuning' can lead to improved accuracy, the asymptotic rates of convergence are no better than those for $\alpha = 1$. In addition, proper selection of α may not always be clearcut. A detailed analysis may reveal a simple and effective method for choosing α, but the results obtained to date for $\alpha = 1$ have been satisfactory.

Similar results to those in Table I are shown in Table II for TRIA3 results normalized with respect to those for the stable MINI element. The MINI element is a P1-P1 element with the

Table II. Solution errors for TRIA3 stabilized element normalized with respect to results for the stable MINI element.

$1/h$	$e^h_{uL_2}$	$e^h_{uH_1}$	$e^h_{pL_2}$	e_{div}
8	0.892	0.985	0.588	0.976
16	0.890	0.996	0.583	0.976
32	0.889	1.000	0.565	0.976
40	0.889	1.001	0.556	0.976
48	0.889	1.001	0.549	0.976
56	0.889	1.001	0.542	0.976

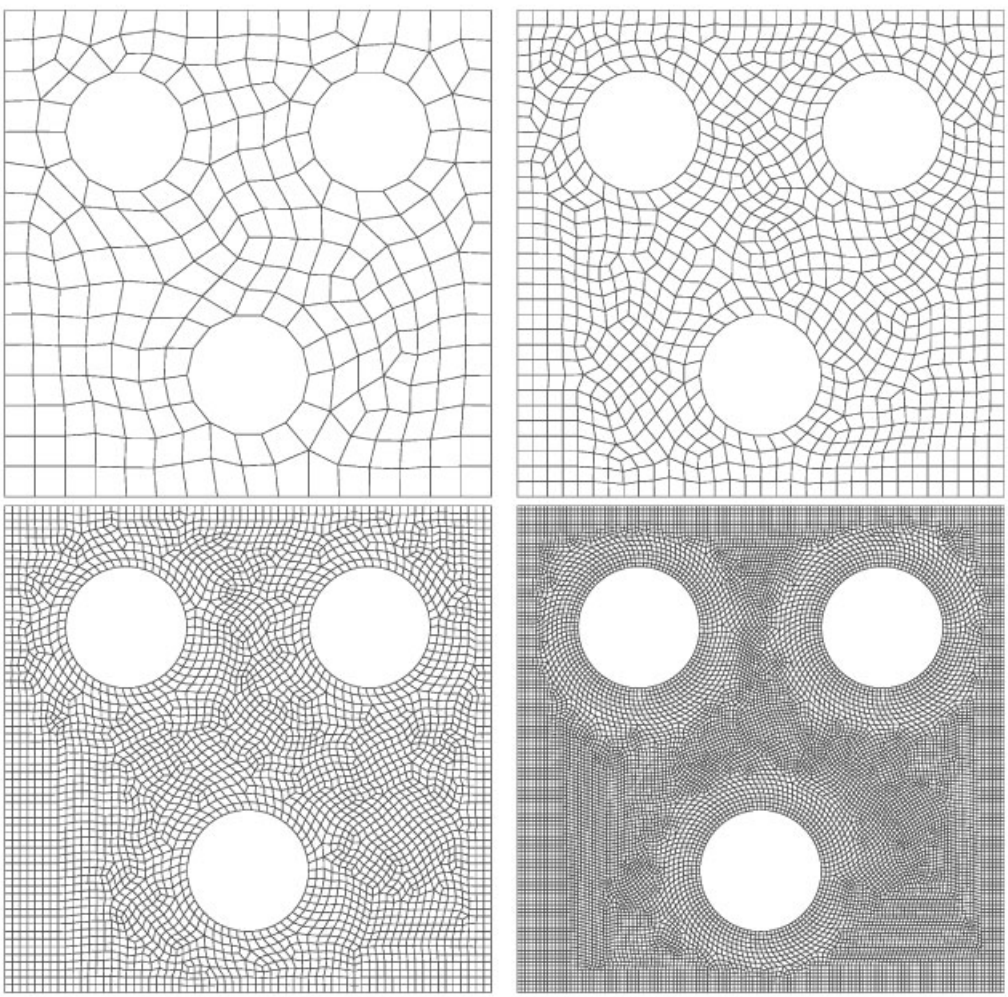

Figure 2. QUAD4 finite element meshes used for second example.

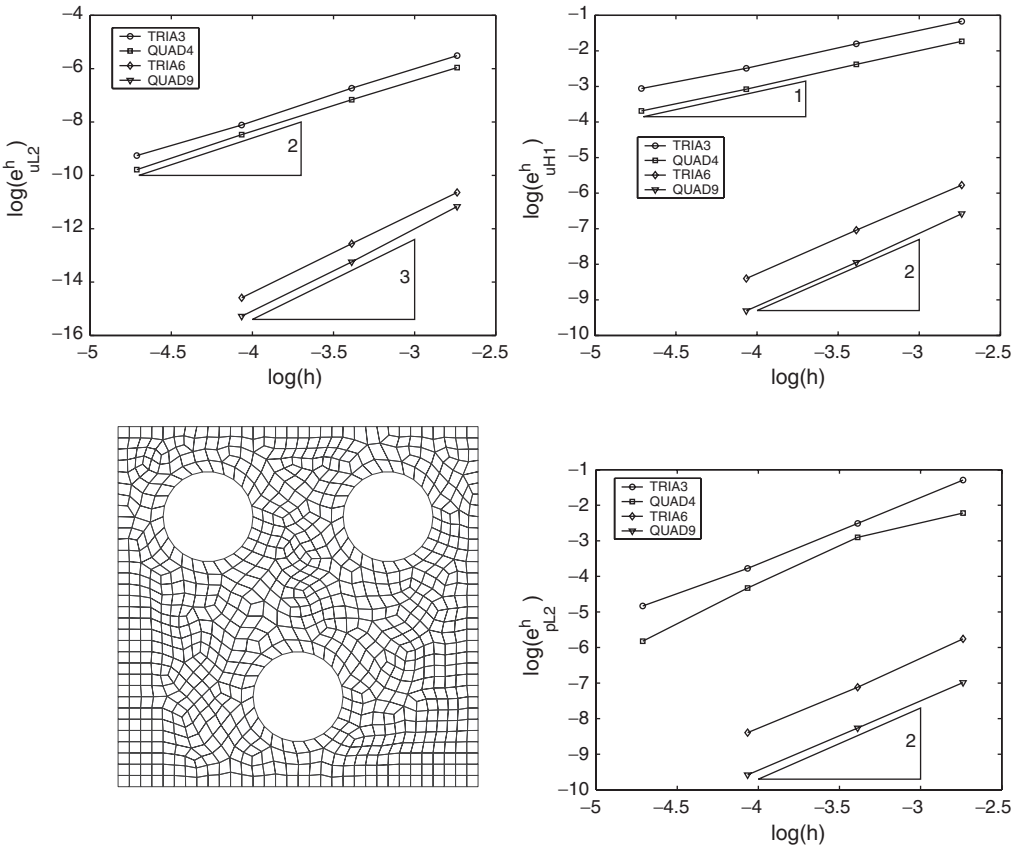

Figure 3. Example quadrilateral mesh and error norms for second example.

velocity field enriched by the cubic bubble. For a description of the Taylor–Hood and MINI elements, see e.g. Reference [25]. The stabilized TRIA3 element has slightly better pressure accuracy than the MINI element for this example.

The second example uses the same exact solution, but now the square domain has three circular cutouts. Note that it is necessary to adjust the constant value of $\frac{4}{3}$ in (49) to satisfy (51). The four QUAD4 meshes used in this example are shown in Figure 2. Meshes for the other 2D element types were obtained from the QUAD4 meshes by adding nodes and splitting elements as needed. Plots of the error norms for the different element types along with an example mesh are shown in Figure 3. In this figure, $h_e = 1/\sqrt{N_e}$ where N_e is the number of quadrilateral elements in the mesh. As expected, the error norms become smaller as the meshes are refined.

The third example has all velocities constrained to zero on the boundary of a unit square. In addition, a concentrated load in the direction $(1, -1)$ is applied to the centre node. The calculated velocities and pressures are shown in Figure 4 along with the QUAD4 finite element

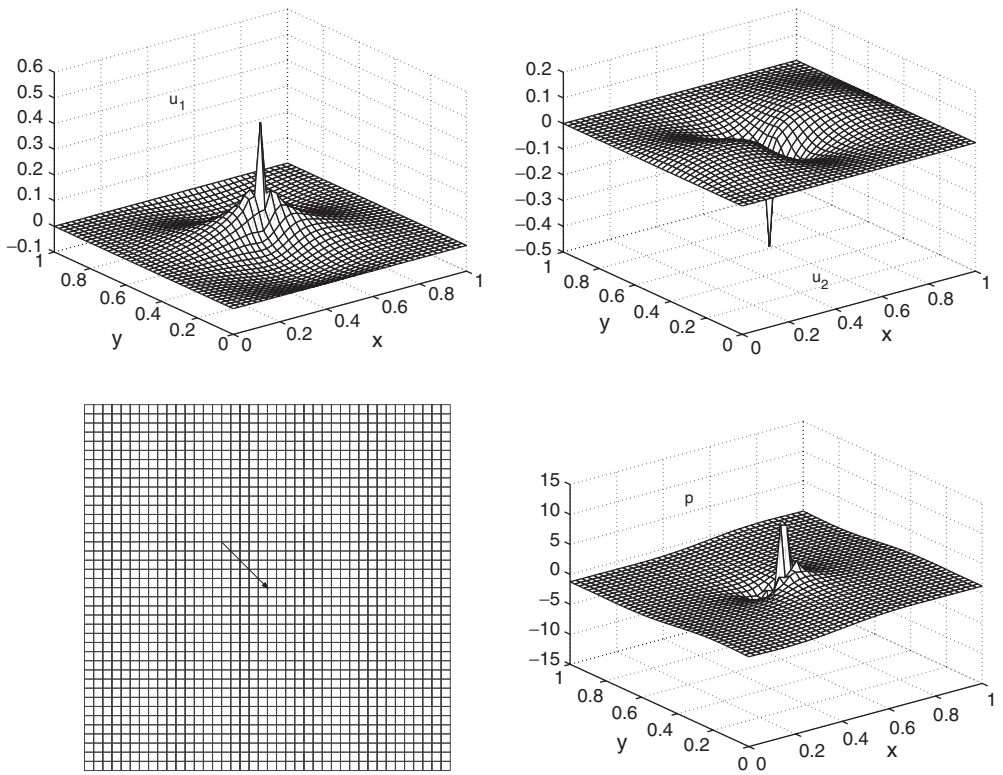

Figure 4. Mesh and calculated responses for concentrated load applied at centre of mesh for third example.

mesh. The purpose of this example is to demonstrate that a point singularity does not cause velocity or pressure oscillations throughout the entire mesh. Although not shown, similar results were obtained for the other three 2D element types.

The final example is for a unit cube with $v = 1$ and the smooth exact solution

$$u_1 = x + x^2 + xy + x^3 y \tag{53}$$

$$u_2 = y + xy + y^2 + x^2 y^2 \tag{54}$$

$$u_3 = -2z - 3xz - 3yz - 5x^2 yz \tag{55}$$

$$p = xyz + x^3 y^3 z - \tfrac{5}{32} \tag{56}$$

The values of **u** on the boundary of the cube are constrained to those given by (53)–(55) and the constant pressure mode is removed by the constraint in (51). As before, **f** is obtained by substituting the exact solution into (6).

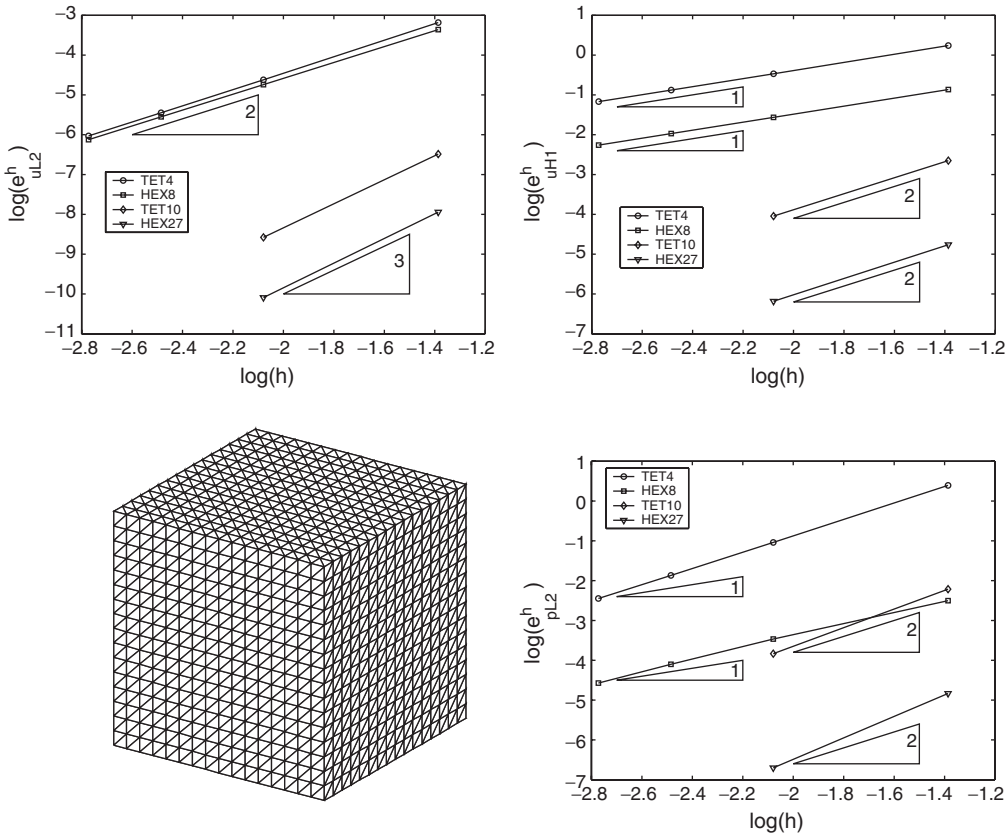

Figure 5. Example tetrahedral mesh and error norms for final example.

Plots of the error norms versus element length are shown in Figure 5. An example tetrahedral mesh is also shown in the figure. As was the case for the 2D example, the convergence rates for $e^h_{uL_2}$ and $e^h_{uH_1}$ coincide with the optimal rates for $k=1$ and $k=2$ given in (45) and (46), respectively. Again, for $k=1$, that is for TET4 and HEX8 elements, the line segment slopes for $e^h_{pL_2}$ are greater than 1. Only two data points for the TET10 and HEX27 elements could be calculated because of computer memory limitations. Nevertheless, when $k=2$ the slopes are closer to the values indicated by (46).

As a final comment, the pressures at two corners for the TET10 mesh were constrained according to (56) in this example. No constraints on pressures other than (51) were made for the other three element types. The reason for doing this for the TET10 mesh is as follows. The number of elements containing nodes with co-ordinates $(1,1,0)$ and $(0,0,1)$ equals one. In addition, the velocity degrees of freedom of the two elements containing these nodes are all constrained. As a result, there are two zero eigenvalues in addition to the zero eigenvalue for the constant pressure mode. This is related to the fact that there are four zero eigenvalues for a single TET10 element with all of its velocity degrees of freedom

constrained. The situation is identical for a similarly constrained stable P2-P1 Taylor–Hood element.

5. CONCLUSIONS

A new stabilized mixed method for the incompressible Stokes equations is proposed and tested numerically. Rather than using the residual of the momentum equation, our method accomplishes stabilization by penalizing the attendant velocity–pressure mismatch in equal-order finite element approximations. As a result, the new method has several important computational properties, including a completely local implementation. It also leads to symmetric linear systems and does not require choice of a mesh-dependent stabilization parameter or calculation of second-order derivatives. Numerical examples presented in this paper demonstrate the very good stability and accuracy properties of the new method.

ACKNOWLEDGEMENTS

The authors wish to thank Max Gunzburger for his helpful comments. Sandia is a multiprogram laboratory operated by Sandia Corporation, a Lockheed-Martin Company, for the United States Department of Energy's National Nuclear Security Administration under contract DE-AC-94AL85000.

REFERENCES

1. Girault V, Raviart P. *Finite Element Methods for Navier–Stokes Equations*. Springer: Berlin, 1986.
2. Brezzi F. On existence, uniqueness and approximation of saddle-point problems arising from Lagrange multipliers. RAIRO Model. *Revue Français D' Autimatique Informatique* 1974; **21**:129–151.
3. Gunzburger M. *Finite Element Methods for Viscous Incompressible Flows*. Academic: Boston, 1989.
4. Baiocchi C, Brezzi F. Stabilization of unstable numerical methods. *Proceedings of the Problemi attuali dell' analisi e della fisica matematica*, Taormina, 1992; 59–64.
5. Hughes TJR, Franca LP, Balestra M. A new finite element formulation for computational fluid dynamics: V. Circumventing the Babuska–Brezzi condition: A stable Petrov–Galerkin formulation of the Stokes problem accommodating equal-order interpolations. *Computer Methods in Applied Mechanics and Engineering* 1986; **59**:85–99.
6. Hughes TJR, Franca LP. A new finite element formulation for computational fluid dynamics: VII. The Stokes problem with various well-posed boundary conditions: symmetric formulations that converge for all velocity pressure spaces. *Computer Methods in Applied Mechanics and Engineering* 1987; **65**:85–96.
7. Douglas J, Wang J. An absolutely stabilized finite element method for the Stokes problem. *Mathematics of Computation* 1989; **52**:495–508.
8. Behr M, Franca L, Tezduyar T. Stabilized finite element methods for the velocity-pressure-stress formulation of incompressible flows. *Computer Methods in Applied Mechanics and Engineering* 1993; **104**:31–48.
9. Becker R, Braack M. A modification of the least-squares stabilization for the Stokes equations, Report 03/00 (2000), University of Heidelberg, http://gaia.iwr.uni-heidelberg.de/Publications/publications.html
10. Bochev P, Gunzburger M. An absolutely stable Pressure–Poisson stabilized method for the Stokes equations. *SIAM Journal on Numerical Analysis*, to appear.
11. Jansen K, Collis S, Whiting C, Shakib F. A better consistency for low-order stabilized finite element methods. *Computer Methods in Applied Mechanics and Engineering* 1999; **174**:153–170.
12. Barth T, Bochev P, Gunzburger M, Shadid JN. A Taxonomy of consistently stabilized finite element methods for the Stokes problem. *SIAM Journal on Scientific Computing* 2004; **25**(5):1585–1607.
13. Blasco J, Codina R. Stabilized finite element method for the transient Navier–Stokes equations based on a pressure gradient projection. *Computer Methods in Applied Mechanics and Engineering* 2000; **182**:277–300.
14. Blasco J, Codina R. Space and time error estimates for a first-order, pressure stabilized finite element method for the incompressible Navier–Stokes equations. *Applied Numerical Mathematics* 2001; **38**:475–497.
15. Codina R, Blasco J. Analysis of a pressure stabilized finite element approximation of the stationary Navier–Stokes equations. *Numerische Mathematik* 2000; **87**:59–81.

16. Silvester DJ, Kechkar N. Stabilized bilinear-constant velocity-pressure finite elements for the conjugate gradient solution of the Stokes Problem. *Computer Methods in Applied Mechanics and Engineering* 1990; **79**:71–86.
17. Silvester D. Optimal low order finite element methods for incompressible flow. *Computer Methods in Applied Mechanics and Engineering* 1994; **111**:357–368.
18. Falk R. An analysis of the penalty method and extrapolation for the stationary Stokes equations. In *Advances in Computer Methods for Partial Differential Equations*, Vichnevetsky R (ed.). AICA: New Brunswick, NJ, 1975; 66–69.
19. Hughes TJR, Liu W, Brooks A. Finite element analysis of incompressible viscous flows by the penalty function formulation. *Journal of Computational Physics* 1979; **30**:1–60.
20. Johnson C, Pitkaranta J. Analysis of mixed finite element methods related to reduced integration. *Mathematics of Computation* 1984; **42**:9–23.
21. Oden TJ. RIP-Methods for Stokesian flow. In *Finite Elements in Fluids*, Vol. 4, Gallagher RH, Norrie DH, Oden JT, Zienkiewicz OC (eds). Wiley: Chichester, 1982; 305–318.
22. Bochev P, Dohrmann C, Gunzburger M. An analysis of a polynomial pressure projection stabilized method for the Stokes equations. *SIAM Journal on Numerical Analysis* (submitted).
23. Ciarlet P. The finite element method for elliptic problems. *SIAM Classics in Applied Mathematics*, Society for Industrial and Applied Mathematics, Philadelphia, PA, 2002.
24. Schunk PR, Heroux MA, Rao RR, Baer TA, Subia SR, Sun AC. Iterative solvers and preconditioners for fully-coupled finite element formulations of incompressible fluid mechanics and related transport problems, Sandia National Laboratories, *Technical Report* SAND2001-3512J, 2002.
25. Bathe KJ. *Finite Element Procedures*. Prentice-Hall: Upper Saddle River, New Jersey, 1996.

